High-Performance Algorithms for Drift Avoidance and Fast Tracking in Solar MPPT System

Ashish Pandey, *Member, IEEE*, Nivedita Dasgupta, and Ashok Kumar Mukerjee, *Member, IEEE*

***Abstract*—The power available at the output of solar arrays keeps changing with solar insolation and ambient temperature. Expensive and inefficient, the solar arrays must be operated at maximum power point (MPP) continuously for economic reasons. Of the numerous algorithms for this purpose, perturb and observe (P&O) is a standard. A derivative of gradient ascent method used in the optimization theory, this algorithm introduces a tradeoff between tracking and dynamic performance. This algorithm also has a tendency to drift the system away from the MPP as atmospheric conditions change. With continually changing atmospheric conditions, these inadequacies lead to poor utilization of solar arrays. This paper addresses both the issues. A variable-step-length algorithm is proposed to eliminate the tradeoff. The drift is minimized by evaluating the entire trend in a power versus voltage curve. Analytical results, validated on a prototype system show excellent performance.**

***Index Terms*—DC-DC power conversion, energy conversion, maximum power point tracking.**

I. Introduction

SOLAR energy is a clean, a maintenance-free, and an abundant source of energy. However, there are some drawbacks: the installation costs of solar panels is high and conversion efficiency is low. Therefore, to make it viable, it becomes essential to maximize the utilization of the arrays. The utilization of solar photovoltaic (PV) cells is hampered by the fact that the power versus voltage (*P–V*) curve in solar cells has a unique maxima at a particular operating voltage. Moreover, the peak available power keeps changing with solar insolation and ambient temperature. Maximum power point trackers (MPPTs) are, therefore, employed to track this peak power and convey it to the load at all times. An MPPT is basically a dc–dc converter whose duty cycle is adjusted for drawing the correct amount of current so that the system operates at the MPP. A block diagram of the system is shown in Fig. 1. The operation of MPPT is fairly straightforward, the operating voltage and current are sensed and fed to the control unit for the computation of duty cycle corresponding to the optimal instantaneous operating point.

Of the several algorithms proposed in the literature for an optimal adjustment of the duty cycle, the most popular technique is the real-time realization of the gradient following method termed perturb and observe (P&O) algorithm [1] and used extensively for the MPPT [2]– [7].

Manuscript received October 30, 2006; revised March 12, 2007. Paper No. TEC-00502-2006.

A. Pandey is with the Nitya Power Technologies Pvt., Ltd., New Delhi 110026, India (e-mail: ashish@ieee.org).

N. Dasgupta and A. K. Mukerjee are with the Centre for Energy Studies, Indian Institute of Technology Delhi, New Delhi 110016, India (e-mail: dasguptanivedita@yahoo.co.in; akmj@ces.iitd.ernet.in).

Digital Object Identifier 10.1109/TEC.2007.914201

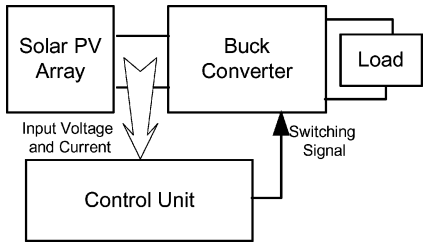

Fig. 1. Block diagram of the MPPT system.

The P&O algorithm [2] has the advantage of simple software and hardware realization. In this pioneering implementation, the reference voltage ($V_{\rm ref}$) is perturbed in an arbitrary direction and the power levels of two consecutive samples are compared. Depending upon the sign of the power change, the direction for further perturbation is decided. A feedback control loop ensures that the output voltage tracks its reference. The following equation is followed to locate the voltage at which the MPP is reached

$$V_{\rm ref}(k) = V_{\rm ref}(k-1) \pm C \tag{1}$$

where k and $k-1$ are the present and the previous instants, and C is the constant search step.

In MPPT systems, the power versus duty cycle (*P–D*) curve also has a maxima at some duty cycle D corresponding to the MPP. This result has been used for searching the MPP [3] by changing the duty cycle according to the following equation.

$$D(k) = D(k-1) \pm C. \tag{2}$$

The previous scheme is greatly simplified by directly manipulating the duty cycle instead of an indirect manipulation by adding a voltage control loop.

Essentially, any implementation of the P&O algorithm including the two basic implementations discussed earlier will inherit the dynamics versus tracking tradeoff. Large step size "*C*" in the aforementioned equations leads to oscillations at the steady-state and continuous power loss, while a reduction in the step size impairs the dynamics of the converter and leads to poor utilization of the solar cells.

This tradeoff is evident from Fig. 2, which shows the startup of the tracker at a different step size. The step size is inferred from the power trace and is indicated by ΔD in Fig. 2. It is observed that, when the step size is 1.4%, the time taken to reach a steady state near the MPP is very long but steady-state oscillations are minimized. On the other hand, if the step size is increased to 2.6%, the system latches up to MPP very quickly, but there is a considerable amount of steady-state power loss due to continuous oscillations. Optimized step size, in terms of

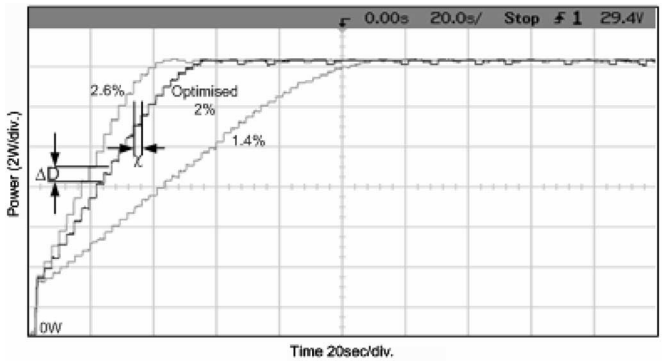

Fig. 2. Startup and steady-state performance of P&O algorithm at $C = 1.4\%$, at $C = 2.6\%$, and optimized at step size of 2%. Power trace obtained from math function of DSO.

tracking time and power drawing capabilities, is found, by trial and error, to be 2%. To take care of this tradeoff, variants of the classical P&O have been proposed by introducing variable search steps [4]. The algorithm is given as

$$V_{\rm ref}(k) = V_{\rm ref}(k-1) \pm M\frac{\Delta P}{\Delta V} \tag{3}$$

where the parameter M is the scaling factor, tuned at design time to scale the step size.

Variable search step can also be evaluated from the slope of the *P–D* curve [5]. This is given by

$$D(k) = D(k-1) \pm M\left|\frac{\Delta P}{\Delta D}\right| \tag{4}$$

where ΔD is the step change in the duty cycle and M is the scaling factor.

One of the difficulties faced in the implementation of variable step size algorithms is in finding the right value of the scaling factor M. This parameter has a significant effect on the performance of the MPPT and requires *ad hoc* tuning measures. The selection of M for an optimal startup at different insolation levels is also not possible. A poor choice of M can easily lead to instability or inefficient tracking during startup and operation at different insolation levels. Moreover, M has to be tuned for each individual system making commercial exploitation of the algorithm prohibitively complicated.

Steady state oscillations at MPP can be eliminated by evaluating power at multiple operating points. Modifications to P&O algorithm have been proposed to evaluate the previous history of operating points [6] or perturbation and evaluation of multiple operating points to identify oscillations [7], [8]. These techniques, albeit simple, do not address the issue of tradeoff directly.

To handle diverse requirements at startup and steady state, hybrid algorithms have also been proposed to improve startup dynamics [9], [10]. These techniques require somewhat complex computation to bring the system to a region near the MPP and then, allow conventional algorithms to take over and gradually bring the operating point to the MPP.

Another drawback of all algorithms in which instantaneous power level is evaluated to decide search direction [2]– [10] is drift. During changing atmospheric conditions, these algorithms allow the operating point to drift away from the MPP [1]. This problem is addressed by the incremental conductance (IncCond) method [11]. IncCond algorithm locates the MPP by searching for an operating point where the following equation holds.

$$\frac{dI}{dV} = -\frac{I}{V}. \tag{5}$$

Claimed to be a more advanced algorithm, its hardware and software implementation is reasonably complex. The condition given by (5) is rarely met in practical situations, and thus, it seldom reaches the exact MPP. Though IncCond is considered superior to all others, it has been shown that the efficiency of the P&O algorithm is approximately equal to the more complex IncCond algorithm [1]. Drift condition has also been addressed in [12]; here, the sampling time is manipulated according to the dynamics of the converter system. Although more accurate, this requires the calculation and knowledge of the intrinsic transient oscillation time of the system. In the actual implementation, design time tunable parameters have to be introduced and dynamics versus steady-state tradeoff has to be satisfactorily addressed. Moreover, a variable sampling frequency will make scheduling of MPPT algorithms in processors difficult in a multitasking system.

It is important, at least for small and medium power applications, that MPPT algorithms are evaluated in the context of applications such as grid interactive inverter and power conditioners, etc. [13]. In a typical digital realization, MPPT algorithms have to vie for processor time along with other tasks such as those controlling inverter. It is, therefore, imperative to design and evaluate MPPT algorithms considering constrain in their scheduling. The periodicity of the MPPT task (χ in Fig. 2) is an important design parameter considering that the MPPT task has to be scheduled according to some viable scheduling protocol.

In this paper, novel techniques are proposed to eliminate drift condition and dynamics versus tracking tradeoff. Strategies are also proposed to automate tuning parameters such as C and M [see (1)–(4)], which simplifies the design of the MPPT. The proposed algorithms are implemented using a software architecture that readily extends to multitasking environment to allow the performance evaluation of proposed algorithms as part of a larger power processing system.

II. Mathematical Modeling and Analysis of the MPPT System

The block diagram of the full MPPT system is shown in Fig. 1. This section deals with the mathematical modeling and analysis of the various components.

A. Solar Cell

The solar cell has a nonlinear relationship between its output voltage and current. The values of these parameters depend upon solar irradiance and cell temperature as given in the following

equation [14].

$$I = I_L - I_{OS}\left\{\exp\left[\frac{q(V+IR_S)}{AkT}\right]-1\right\} - \frac{V}{R_{SH}}. \quad (6)$$

In the aforementioned equation, *I* is the output current of the solar cell, I_L is the current across the p-n junction (light generated current—this parameter depends upon the solar insolation), I_{OS} is the reverse saturation current of cell, q is the electronic charge, V is the output voltage of the cell, R_S stands for the series resistance (ideally zero), *A* is the ideality factor, k denotes the Boltzmann's constant, and *T* is the absolute operating temperature. R_{SH} denotes the shunt resistance, which is ideally infinity, and therefore, last term in (6) is generally dropped.

B. Buck Converter Analysis

In a buck converter, the duty cycle D, i.e., the ratio of "ON" time to total time period is given as [15]

$$D = \frac{V_O}{V} \quad (7)$$

where V and V_O are the input and output voltage of the buck converter.

The buck converter and the load present an equivalent load on the solar array system. This equivalent resistance has to be same as R_s of the solar cell to achieve maximum power transfer. The equivalent load resistance of the converter can be derived from the model of buck converter and can be given as

$$R_{\rm eq} = \frac{\eta R_L}{D^2} \quad (8)$$

where η and R_L are the converter efficiency and load resistance, respectively.

The MPPT algorithm can directly adjust the duty cycle *D* to match the load impedance $R_{\rm eq}$ to source impedance R_s, according to (8).

From the solar cell equation and (8), the dependency of panel current and power upon the converter duty cycle are given by the following equations.

$$I = I_{\rm L} - I_{\rm O}\left\{\exp\left[\frac{q\eta R_{\rm L} I}{AkTD^2}\right]-1\right\} \quad (9)$$

and

$$P = I_{\rm L}\left(\frac{I\eta R_{\rm L}}{D^2}\right) - I_{\rm O}\left(\frac{I\eta R_{\rm L}}{D^2}\right) \times\left\{\exp\left[\frac{q\eta R_{\rm L} {\rm I}}{AkTD^2}\right]-1\right\} \quad (10)$$

Equations (8)–(10) correspond well with normalized empirical data on variation of panel power, voltage, current, and circuit equivalent resistance with *D*, as shown in Fig. 3(a) and (b).

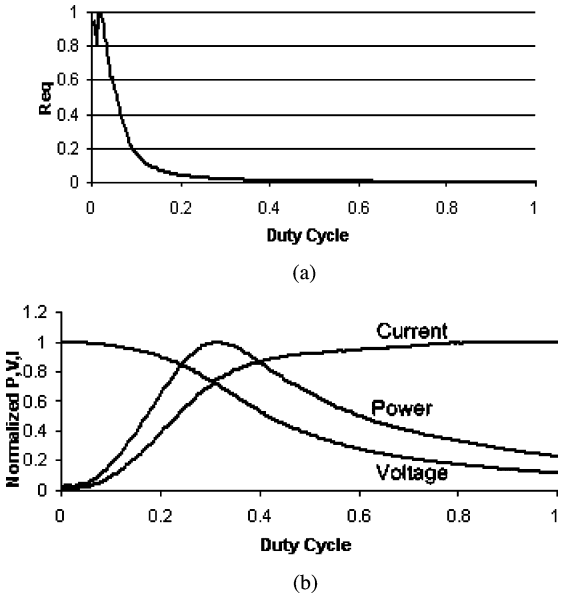

Fig. 3. (a) Experimental curve showing the inverse proportionality of $R_{\rm eq}$ with the square of the duty cycle. (b) Variation of panel current, voltage, and power with duty cycle of the dc–dc converter.

III. Analysis of Proposed Algorithms

The algorithms proposed in this section have been designed to address the following shortcomings of the standard P&O algorithm:

1) eliminate dynamics versus tracking tradeoff;
2) eliminate all *ad hoc* parameters that require tuning at design time;
3) eliminate drift.

A. Delta P&O Algorithm

In Delta P&O algorithm, the duty cycle is perturbed to locate optimal operating point corresponding to the MPP. dP/dV is used to evaluate variable step size and tuning of scaling parameter *M* [see (3) and (4)] is automated.

1) Variable Step-Size Parameter: As discussed in Section I, the step size in the P&O algorithm is a critical design parameter, which requires design time tuning to strike a balance between dynamics and steady-state behavior of the system.

Study of experimental *P–D* and *P–V* curves and their derivatives (Fig. 4) indicate that the derivatives are uniquely suitable for step size after proper scaling. They meet the requirement for the step size, which should ideally be large when the operating point is away from the MPP, and monotonically decrease as the MPP is approached.

From the results shown in Fig. 4(a) and (b), it is clear that the derivative of power w.r.t. voltage varies more smoothly as compared to the derivative of power w.r.t. duty cycle (when taken against duty cycle). Therefore, it may be emphasized that $\Delta P/\Delta V$ is a better-suited parameter for deciding step size as compared to $\Delta P/\Delta D$. Thus, in the present system, $\Delta P/\Delta V$ is used as the scaling parameter for the step change in the duty cycle. The Delta P&O algorithm is proposed and it is depicted by the following equation:

$$D(k+1) = D(k) \pm M\frac{|P(k)-P(k-1)|}{|V(k)-V(k-1)|} \quad (11)$$

2) Removing Ad Hoc Methods of Determining M: Scaling factor *M* in (11) essentially decides the performance of the

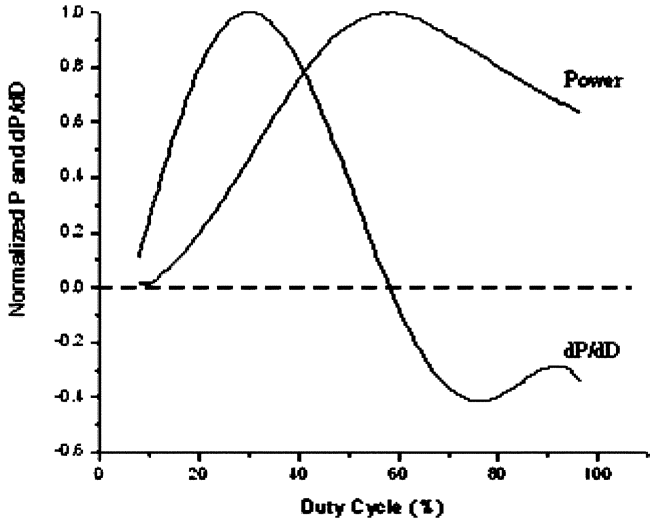

(a)

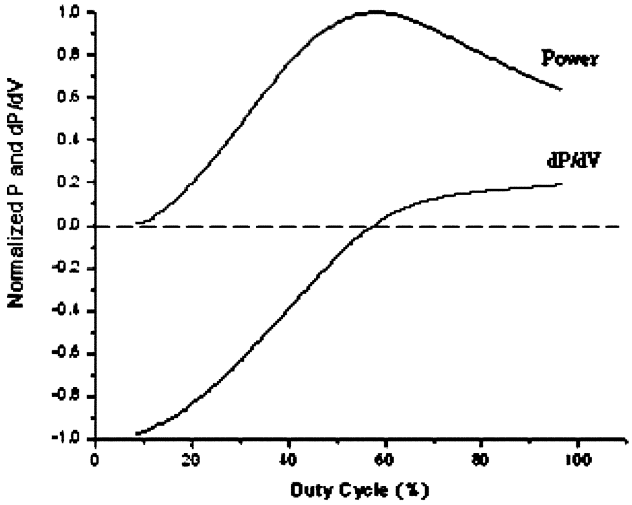

(b)

Fig. 4. Approximated and normalized empirical curves. (a) *P* and the derivative of *P* w.r.t. *D*. (b) *P* and the derivative of *P* w.r.t. *V*. These are plotted against the control parameter *D*. Curve (a) shows erratic variation of the derivative whereas (b) shows smooth variation. The observations were taken from single *PV* panel at an insolation level of 620 W/m^2 at 2.20 P.M. on a clear day in the month of May in New Delhi, India.

MPPT system. Manual tuning of this parameter shows that it is extremely sensitive to initial operating conditions. A fixed value of *M* tuned under certain insolation condition will fail to give satisfactory performance or even lead to instability when operated under different insolation level. To ensure satisfactory operation under all startup conditions, it is essential that *M* be automatically tuned during initialization process at the startup.

For automatically tuning parameter *M*, the duty cycle D_{start} is initialized to a low value. Power P_{start} and voltage V_{start} are evaluated at this duty cycle. Subsequently, duty cycle is changed by maximum safe step change $\Delta D_{\max}$ and corresponding values of $\Delta P_{\max}$ and $\Delta V_{\max}$ are evaluated. From (11)

$$\Delta D_{\max} \equiv M \frac{|\Delta P_{\max}|}{|\Delta V_{\max}|} \tag{12}$$

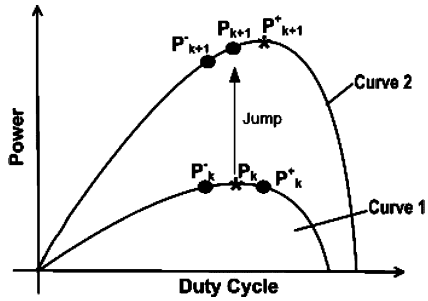

Fig. 5. FulCurvE evaluation algorithm.

$$M = \frac{|\Delta V_{\max}|\,\Delta D_{\max}}{|\Delta P_{\max}|}. \tag{13}$$

The pseudocode for calculating *M* at startup can be given as

$$//Initialisation\ \ routine$$
$$MaxDuty = Maximum\ \ Step\ Size$$
$$StartDuty = Initial\ Duty\ Cycle$$
$$DutyCycle = StartDuty//Start\ Converter$$
$$Sample\ V(k), I(k); p(k) = V(k)I(k)$$
$$DutyCycle = StartDuty\ +\ MaxDuty$$
$$SampleV(k+1), I(k+1), P(k+1) = V(k+1)I(k+1)$$
$$DeltaPower = |P(k+1) - P(k)|$$
$$DeltaVoltage = |V(k+1) - V(k)|$$
$$M = DeltaVoltage\ *\ MaxDuty/DeltaPower$$

Since dP/dV has a maximum value at startup and also as evident from the aforementioned pseudocode, *M* calculated through (13) gets an appropriate minimal value at the startup, and thus, prevents blowing up of the second term of (11) to large values subsequently. This, in turn, prevents huge oscillations around the MPP at steady-state conditions. Also, autotuning of this parameter gives efficient overall steady-state and dynamic performance irrespective of the source (panel/array) and the atmospheric condition at the start up and simplifies design of the MPPT considerably.

B. Full Curve Evaluation (FulCurvE) Algorithm

The problem of drift stems from algorithmic deficiency. The evaluation of a single point in the *P–V* curve at each sampling interval can easily lead to drift when the atmospheric conditions are changing (see [1] for a detailed description on the phenomena).

As shown in Fig. 5, at the sampling instant *k*, the power is evaluated at the duty cycle D_k. Subsequently, the duty cycle is perturbed by $\pm\Delta D$ to get the corresponding power levels P_{k+} and P_{k-}. In case of change in insolation level between successive sampling runs, the operating point automatically jumps to the corresponding point in the new curve. In the next sampling run, all the three points are identified to evaluate the shape of

the curve at the new operating point. Since the complete trend in the *P–D* curve is evaluated before deciding the search direction, drift is completely avoided. An important point to be considered here is that the step size for evaluation of the curve need not to be of size similar to step size for the next jump. The curve can also be evaluated at much smaller step size. Pseudocode for FulCurvE algorithm can be given as

$$Sample\ Pk, Pk+, Pk-$$
$$If\ (Pk- < Pk\ AND\ Pk <= Pk+)$$
$$D = D\ +\ \Delta D$$
$$OR$$
$$If(Pk- >= Pk\ AND\ Pk\ > Pk+)$$
$$D = D - \Delta D$$
$$ELSE$$
$$No\ \ Change$$

Evidently, two sampling frequencies come into play in this algorithm. At each call to the FulCurvE algorithm, the sampling of $(P_{\rm k}, P_{\rm k+}, P_{\rm k-})$ must be carried at rate faster than the dynamics of atmospheric change. This sampling frequency does not decide the periodicity of scheduling of the MPPT task in a multitasking system, which is the time period between successive calls for the FulCurvE algorithm.

In the final form, the Delta P&O and FulCurvE algorithms are combined to present a hybrid algorithm to avoid drift while eliminating tradeoff between dynamics and steady-state oscillations. In the hybrid algorithm, D and ΔD in the aforementioned pseudocode are evaluated and updated according to (11). In another variant, the hybrid algorithm is tested with small fixed size steps for curve evaluation while using the Delta P&O algorithm for deciding the jump steps.

IV. MPPT System Description

A prototype of an MPPT system is built to validate the aforementioned analysis. The various hardware components and the software architecture are described next.

A. Hardware Description

A 40-W MPPT system is designed around a buck type dc–dc converter and a microcontroller (μC)-based control unit. The system is experimentally tested on a solar array simulator (SAS) that is used to reproduce single and double (two panels in series) panel *P–V* characteristics.

1) Source: The results are obtained with Agilent SAS E4351B. The experimental results presented in Section V are taken by using the "SAS mode" of this simulator that approximates the actual *PV* curves. The values for setting the curves are obtained from *P–V* and *I–V* characteristics of single 36 W solar panel manufactured by CEL Ltd., New Delhi, India.

2) Buck Converter Specifications: The buck converter parameters are the following.

1) Input voltage range: $7 - 40\,V_{\rm dc}$.

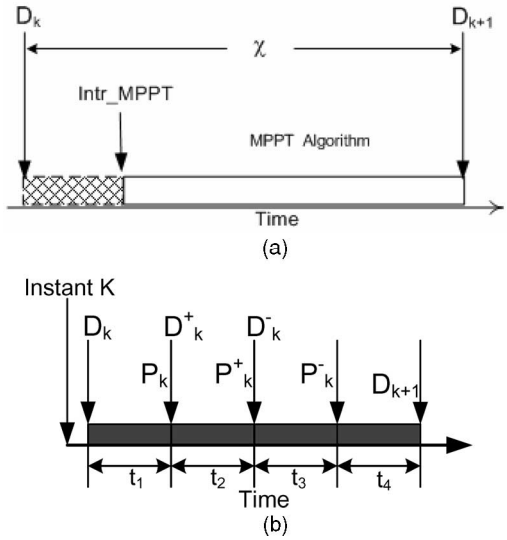

Fig. 6. (a) Scheduling MPPT interrupt for Delta P&O algorithm. (b) Infinite loop scheduling of FulCurvE algorithm.

2) Switching frequency: 10 kHz.
3) Allowed inductor ripple current: 20% of output current.
4) Allowed output voltage ripple: 100 mV peak to peak.
5) Inductor value: 450 μH.
6) Capacitor value: 470 μF.

3) Processor and Interface: The control circuit consists of Hall effect sensors for current and voltage. IR2125MOSFET/IGBT driver IC for triggering the converter switch connected to on-chip pulse width modulation (PWM) peripheral via HCPL2211 optocoupler and buffer circuits. The μC used is Analog Devices ADuC831 with 8052 core. It contains an 8-channel 12-bit ADC, 62 KB program memory, 4 KB data memory, 256 B of RAM and a dual-output 16-bit PWM.

B. Software Architecture

The software architecture for a stand-alone MPPT system can be extremely simple. As discussed earlier, a more viable solution is to control the MPPT as well as the downstream power processor such as inverter using a single processor. This requires that the MPPT be tested on architecture that is capable of accommodating tasks relating to inverter control at a later development stage. The present system is tested on interrupt-based background–foreground architecture. Essentially in this architecture, the background task in an infinite loop that waits for the foreground tasks. The foreground task is a periodic interrupt—intr_MPPT. This task reads the ADCs and runs the MPPT algorithm. The periodicity χ as shown in Fig. 6(a) and also reflected in Fig. 2 (assuming negligible lag between power and control circuit) of the Intr_MPPT task is set to 2.5 s for the present system to allow space for future modifications. Currently, the processor is running idle in the background loop. The current and voltage input signals are averaged over few cycles to remove noise.

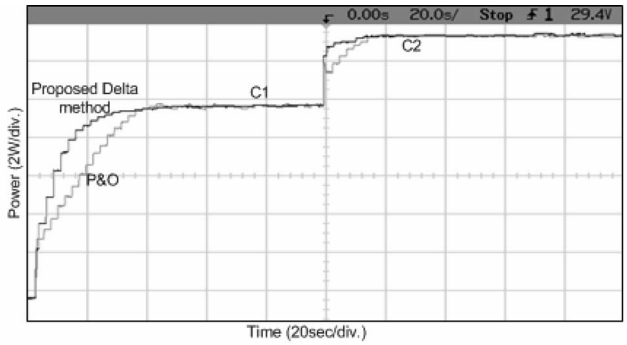

Fig. 7. Comparison of steady-state and dynamic performance of MPPT system with the proposed Delta P&O algorithm with P&O algorithm. SAS settings corresponding to single-panel system are used. *C*1 and *C*2 are at the insolation levels corresponding to maximum powers of 10.0 and 14.0 W, respectively.

The FulCurvE algorithm is tested on infinite loop architecture. The duty cycle is adjusted and power is evaluated in each sampling run. The bandwidth defined in Section III is essentially in terms of time $t_1 + t_2 + t_3$ during which the values of power at the three duty cycles are evaluated. The algorithm runs in time slice t_4 Fig. 6(b).

V. Experimental Results and Discussions

The various algorithms are tested independently to validate the analysis given in Section III. The voltage signal is measured with an isolated voltage probe HP N2772A and the current is measured using current probe HP 1146A and displayed on Agilent 54621A DSO. The HP SAS is used for creating repeatable test conditions. The power trace is displayed through the math function on the digital storage oscilloscope (DSO).

Fig. 7 shows the startup and steady-state waveforms for the MPPT system running on the Delta P&O algorithm given by (11) with automatic tuning of the parameter *M* given by (13) and is compared with the standard P&O algorithm. In the initialization process, an initial step is given to determine *M*. Steady-state oscillations are the very essence of all P&O algorithms [1]. The system is, therefore, tested for step change in the power level after the converter system had stabilized. The new MPP is tracked within a few sampling cycles as shown in Fig. 7. Clearly, the proposed Delta P&O method has faster dynamics and more stable steady state than classical hill-climbing algorithm. As predicted by analysis in Section IV, the system quickly responds to the step change by increasing the step size, which is then quickly reduced when the new MPP is located.

As expected, the ΔD reduces to a naught as the system oscillates around the MPP, thereby achieving the objective of eliminating the tradeoff.

As stated in Section III, there is a necessity of autotuning of the scaling parameter for making the system robust. Fig. 8 shows the comparison between the Delta P&O algorithm with autotuned *M* and that with manually tuned *M* for *P–V* curve with $P_{\max} = 37.5$ W (with SAS settings corresponding to two panel system). Here, the performance of auto and manually tuned values of *M* are comparable. However, when this manually tuned value of the scaling parameter is fixed for all times and for all

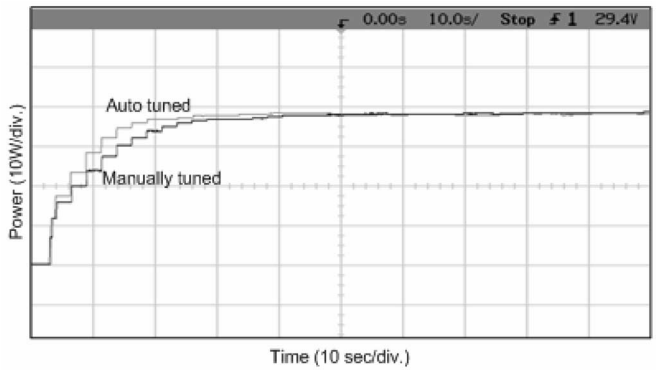

Fig. 8. Performance evaluation of power curves at autotuned and manually tuned value of *M* at startup and steady state at 37.5 W $P_{\max}$.

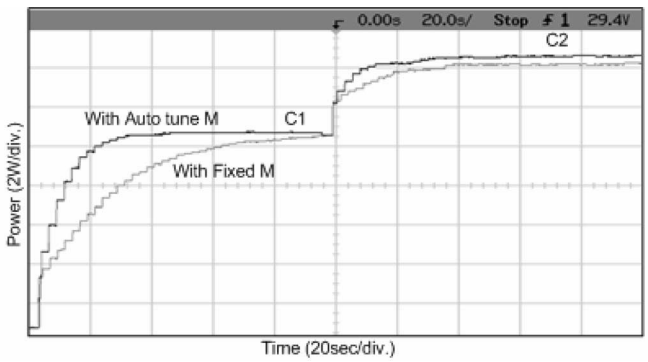

Fig. 9. Startup and steady-state and step change performances of autotuned and manually tuned (for 37.5 W two-panel), i.e., fixed-*M* variable-step-size algorithms. *C*1 and *C*2 are at the insolation levels corresponding to maximum powers of 10.0 and 14.0 W, respectively.

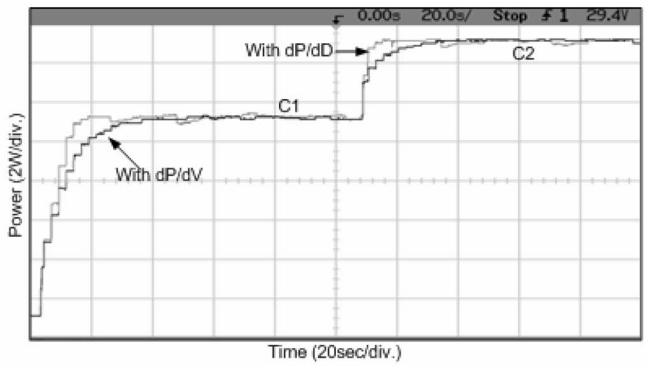

Fig. 10. Performance of autotuned Delta P&O algorithm with dP/dD and dP/dV as step sizes. *C*1 and *C*2 are at the insolation level corresponding to 10.0 and 14.0 W, respectively.

startup conditions, the performance turns out to be poor. This is evident from Fig. 9. It is observed that the Delta P&O algorithm with autotuning of *M* always works better for start ups with a different sources (single panel) or with the same source at a different sets of atmospheric conditions.

As described in Section III, dP/dV is a better-suited parameter than dP/dD for step size. Fig. 10 compares the dynamic and steady-state performance of the proposed Delta P&O algorithm with variable step algorithm where the step size is decided by dP/dD. The proposed algorithm provides a marginally slower

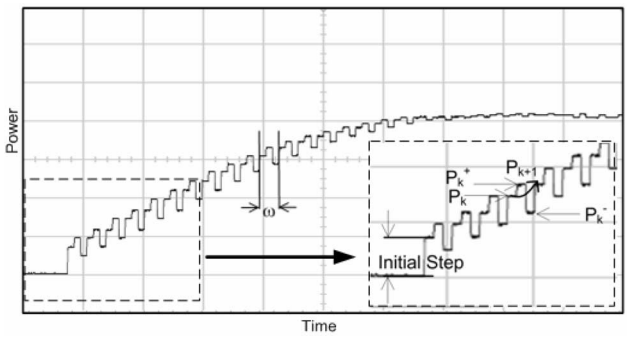

Fig. 11. Startup with FulCurvE algorithm.

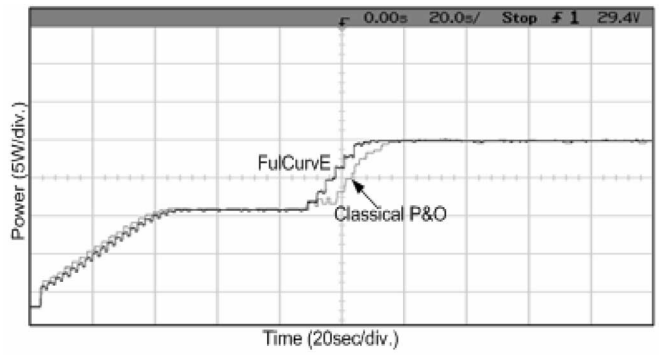

Fig. 12. Startup and dynamic performances of FullCurvE and P&O algorithms under changing atmospheric conditions starting from insolation level corresponding to 12.0 through 22.0 W.

but smoother response during dynamics and a better steady-state performance.

The FulCurvE algorithm is implemented on lines of analysis given in Section III. The power is evaluated at $\pm\Delta D$ at kth and $(k+1)$th sampling instant. As shown in Fig. 11 inset, the power level at $+\Delta D$ is greater than power level at $-\Delta D$. As expected, the algorithm decides the next search direction in the $+\Delta D$ direction. Here, ω is the time taken to evaluate the entire trend in the power curve and essentially decides the robustness or bandwidth of the algorithm. The value of ω is an implementation issue. Here, it is necessary to state that ω should be smaller than expected rate of environmental conditions change.

Testing of the FulCurvE algorithm is done under repeatable changing atmospheric condition created by the SAS. This is done by increasing the MPP power from 12.0 to 22.0 W through multiple steps.

Fig. 12 shows the steady state and dynamic performance under changing atmospheric condition of a fixed step FulCurvE compared to that of classical hill climbing. Here, it can be observed that the classical fixed step P&O drifts away from the MPP. The FulCurvE algorithm, on the other hand, tightly regulates the system along the desired trajectory.

As evident from the analysis given in Section III, in isolation, the Delta P&O algorithm can be used for improving the steady-state and dynamic performance of the MPPT whereas the FulCurvE algorithm eliminates the drift condition. Therefore, a hybrid algorithm is developed that works with the FulCurvE logic and has the step size and *M* adjustment according to the Delta P&O method. In Fig. 13, the dynamic and steady-state

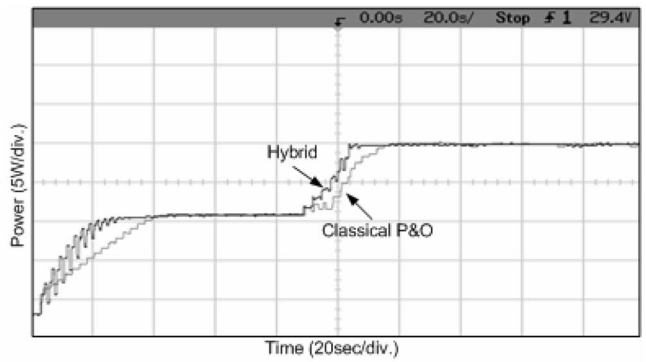

Fig. 13. Steady-state and dynamic performances of hybrid and P&O algorithms under rapidly changing atmospheric conditions starting from insolation level corresponding to maximum power of 12.0 through 22.0 W.

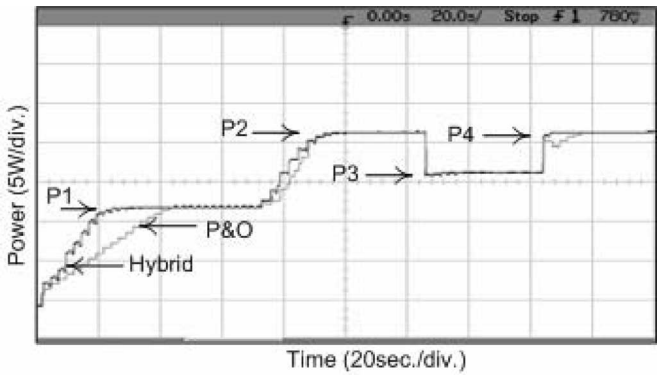

Fig. 14. Comparison of hybrid and P&O algorithm subjected to benchmark loading pattern. Power states *P*1, *P*2, *P*3, and *P*4 correspond to solar conditions with ideal maximum power of 12.0, 21.92, 16.51, and 21.92 W, respectively.

TABLE I
STEADY-STATE MPPT EFFICIENCIES OF THE VARIOUS ALGORITHMS

Algorithm	Efficiency (%)
P&O	98.6
Delta P&O	98.7
FulCurvE	98.75
Hybrid	98.8

performances of P&O and the hybrid algorithm have been compared experimentally. It is observed that this method has faster dynamics, stable steady state, and better performance under changing environmental conditions.

As evident from Fig. 13, straightforward approach of combining FulCurvE and Delta P&O results in large oscillations during startup. These oscillations will also occur during large step changes. A solution to this is use of small fixed step size for curve evaluation. The Delta P&O algorithm decides the jump step size, which defines the dynamics of the system. The results are shown in Fig. 14.

An important figure of merit in evaluating MPPT algorithms is efficiency. This MPP tracking efficiency is a ratio of total power drawn to maximum available power over a period of time [1]. Efficiency of various algorithms during steady state is shown in Table I.

From Table I, it can be seen that the steady-state efficiency values are close to each other. The reasons are that the power curve

TABLE II
MPP TRACKING EFFICIENCIES OF THE VARIOUS ALGORITHMS DURING THE CHANGING CONDITIONS AS SHOWN IN FIG. 14

Algorithm	MPP Tracking Efficiency (%)
P&O	88.1
Delta	92.5
FulCurvE	92.2
Hybrid	94.6

flattens out at its peak, and therefore, an optimal P&O algorithm will essentially have comparable steady-state performance. The efficiency is also influenced considerably by presence of noise and instrument tolerances. While steady-state efficiency of all the algorithms is comparable, such a condition rarely exists in nature for extended period. Therefore, in context of this paper, dynamic efficiency is also evaluated. Due to lack of benchmark, a loading pattern consisting of the three possible dynamic situations viz. startup, step change, which simulates sudden partial or complete shading of the solar panel, and changing atmospheric condition is created. The loading pattern and behavior of hybrid and P&O algorithm is shown in Fig. 14.

The overall MPP tracking efficiencies for the benchmark loading pattern is reported in Table II. This includes the start up, step change, steady state, and the rapidly changing conditions as shown in the full CRO reading in Fig. 14. The Delta algorithm gives a slightly better performance as the benchmark is slightly skewed toward step changes. In this context, startup can also be viewed as a step change. The FulCurvE algorithm provides improvement primarily during drift and in a very limited case during step change as well. The hybrid algorithm gives a consistently better performance during dynamic conditions as well as drift. Both variants of the hybrid and FulCurvE algorithms give comparable performance. When the evaluation step size is decided by the Delta P&O algorithm, the step size becomes negligible during steady state, and therefore, the hybrid algorithm fails to evaluate the complete curve. However, in presence of dynamics, the Delta term quickly builds up the evaluation step size as also evident in Fig. 14, and hence, the algorithm is able to address the drift situation.

VI. CONCLUSION

Algorithms have been proposed and tested to overcome inadequacies of the generic P&O algorithms. A variable step size Delta P&O algorithm is proposed to eliminate dynamics versus tracking tradeoff. By introducing an autotuning mechanism to adjust scaling factor, all *ad hoc* measures required during design time are eliminated. The FulCurvE algorithm evaluates the entire curve at an insolation level, and therefore, can eminently handle drift situation, which occur due to evaluation of instantaneous power by the generic P&O algorithms. Finally, algorithms are integrated to demonstrate a hybrid system and verified using a SAS under repeatable test conditions. Solar MPPTs cater to wide-ranging applications. For rooftop applications, FulCurvE and hybrid algorithms can provide an excellent MPPT solution. In mobile applications, such as automobiles where a chance of intermittent partial or complete shading is possible, Delta P&O and hybrid algorithms can provide a viable solution. Overall, the hybrid algorithm provides an excellent MPPT solution for all types of applications. Future work includes integrating the MPPT system with an inverter system creating opportunities to explore various software architectures to reliably schedule various time critical tasks.

REFERENCES

[1] D. P. Hohm and M. E. Ropp, "Comparative study of maximum power point tracking algorithms," *Prog. Photovolt: Res. Appl.*, vol. 11, pp. 47–62, 2003.
[2] C. Hua, J. Lin, and C. Shen, "Implementation of a DSP-controlled photovoltaic system with peak power tracking," *IEEE Trans. Ind. Electron.*, vol. 45, no. 1, pp. 99–107, Feb. 1998.
[3] E. Koutroulis, K. Kalaitzakis, and N. C. Voulgaris, "Development of a microcontroller-based, photovoltaic maximum power point tracking control system," *IEEE Trans. Power Electron.*, vol. 16, no. 1, pp. 46–54, Jan. 2001.
[4] P. Huynh and B. H. Cho, "Design and analysis of a microprocessor-controlled peak-power-tracking system for solar cell arrays," *IEEE Trans. Aerosp. Electron. Syst.*, vol. 32, no. 1, pp. 182–190, Jan. 1996.
[5] W. Xiao and W. G. Dunford, "A modified adaptive hill climbing MPPT method for photovoltaic power systems," in *Proc. IEEE 35th Annu. Power Electron. Spec. Conf. (PESC 2004)*, vol. 3, pp. 1957–1963.
[6] K. H. Hussein and I. Muta, "Modified algorithms for photovoltaic maximum power point tracking," in *Proc. Joint Conf. Electr. Electron. Eng.*, Kyushu, Japan, Oct.1992, pp. 301–306.
[7] Y.-T. Hsiao and C.-H. Chen, "Maximum power tracking for photovoltaic power system," in *Proc. Ind. Appl. Conf., 2002 Conf. Rec. 37th IAS Annu. Meet.*, vol. 2, pp. 1035–1040.
[8] T. Kawamura, K. Harada, Y. Ishihara, T. Todaka, T. Oshiro, H. Nakamura, and M. Imataki, "Analysis of MPPT characteristics in photovoltaic power system," *Solar Energy Mater. Solar Cells*, vol. 47, no. 1–4, pp. 155–165, Oct. 1997.
[9] S. Jain and V. Agarwal, "A new algorithm for rapid tracking of approximate maximum power point in photovoltaic systems," *IEEE Power Electron. Lett.*, vol. 2, no. 1, pp. 16–19, Mar. 2004.
[10] C. Hua and J. Lin, "A modified tracking algorithm for maximum power tacking of solar array," *Energy Convers. Manage.*, vol. 45, no. 6, pp. 911–925, Apr. 2004.
[11] K. H. Hussein, I. Muta, T. Hoshino, and M. Osakada, "Maximum photovoltaic power tracking: An algorithm for rapidly changing atmospheric conditions," *Proc. IEE Gen., Transmiss. Distrib.*, vol. 142, pp. 59–64, 1995.
[12] N. Femia, G. Petrone, G. Spagnuolo, and M. Vitelli, "Optimization of perturb and observe maximum power point tracking method," *IEEE Trans. Power Electron.*, vol. 20, no. 4, pp. 963–973, Jul. 2005.
[13] B. K. Bose, P. M. Szczesny, and R. L. Steigerwald, "Microcomputer control of a residential photovoltaic power conditioning system," *IEEE Trans. Ind. Appl.*, vol. IA-21, no. 5, pp. 1182–1191, Sep./Oct. 1985.
[14] J. A. Gaw and C. D. Manning, "Development of a photovoltaic array model for use in power-electronics simulation studies," *Proc. IEE Electr. Power Appl.*, vol. 146, no. 2, pp. 193–200, Mar. 1999.
[15] K. Kitsum, *Switch Mode Power Conversion: Basic Theory and Design*. New York: Marcel Dekker, 1984.

Ashish Pandey (M'00) received the B.S. and M.S. degrees in electrical engineering from Tashkent State Technical University, Tashkent, Uzbekistan, in 1997, and the Ph.D. degree from the Indian Institute of Technology (IIT) Delhi, Delhi, India, in 2003.

He is with the ROCSYS Technologies Pvt. Ltd., Hyderabad, India. He is currently engaged in research and product development in high-availability and high-efficiency power electronics for power supplies, power quality, and nonconventional energy sources. His work spans entire power electronics technology from embedded control software, control algorithms to design of high-efficiency and reliable power conversion systems. He is the author or coauthor of more than 25 publications in refereed journals and conferences.

Nivedita Dasgupta received the Graduate degree in physics from the University of Delhi, Delhi, India, in 2001, the M.Sc. degree in physics in 2003 from the Indian Institute of Technology Delhi, Delhi, where she is currently working toward the Ph.D. degree in photovoltaic systems.

Her current research interests include solar maximum power point tracking, nonconventional energy sources, and power electronics.

Ashok Kumar Mukerjee (M'07) received the Undergraduate and Postgraduate degrees in physics and the Ph.D. degree in 1975 from Delhi University, Delhi, India.

He is currently with the Indian Institute of Technology Delhi, Delhi, India. His major contributions are the development of entire technology of photovoltaics from characterization of individual cells to a dual-axis tracking 500 W power generation plant. He has developed a number of technologies for commercial exploitation, some of which have been transferred to several Indian and American firms. He has supervised four Ph.D. and seven M.Tech. theses in photovoltaic instrumentation. He is the author or coauthor of 44 published research papers.